ALTER-EGO

By Gianluca Lentini, Alessandro Settimi, Danilo Caporale,
Manolo Garabini, Giorgio Grioli, Lucia Pallottino,
Manuel G. Catalano, and Antonio Bicchi

Historically, robots first found application in factories and plants. Until recently, the most noticeable examples of robot systems directly sold to the consumer were limited to edutainment systems (e.g., NAO [1]), automated chore robots [26], and social telepresence platforms [27]. Initially, telepresence robots consisted of a mobile base with an interactive screen. Today, following a trend of anthropomorphization of technology, human-like upper bodies have begun to replace those simple screens (e.g., Pepper [2] and R1 [3]) and share the same social communication modalities of humans, e.g., body posture, gestures, gaze direction, and facial expressions. Unfortunately, social robots are mostly designed to speak and make gestures and have limited capabilities when it comes to physically interacting with people and their surrounding environments.

On the other hand, looking at the state of art, there are promising examples (e.g., WALK-MAN [4], Atlas [5], and TORO [6]) of humanoid robots that have been developed to operate in unstructured environments and perform challenging interaction tasks, e.g., walking on rough terrains, moving heavy objects, and solving complex bimanual manipulation tasks. Specific enabling technologies have improved the effectiveness of these robots and facilitate their interactions with the surrounding world, e.g., active impedance control in TORO and series-elastic actuation in WALK-MAN. Indeed, these same technologies permit robot arms to cross the borders of industrial work cells and become the type of collaborative robots that can work in close contact with people and share the same operating space.

Although both humanoid robotics and teleoperation have a long history, we believe that three concurrent factors

A Mobile Robot With a Functionally Anthropomorphic Upper Body Designed for Physical Interaction

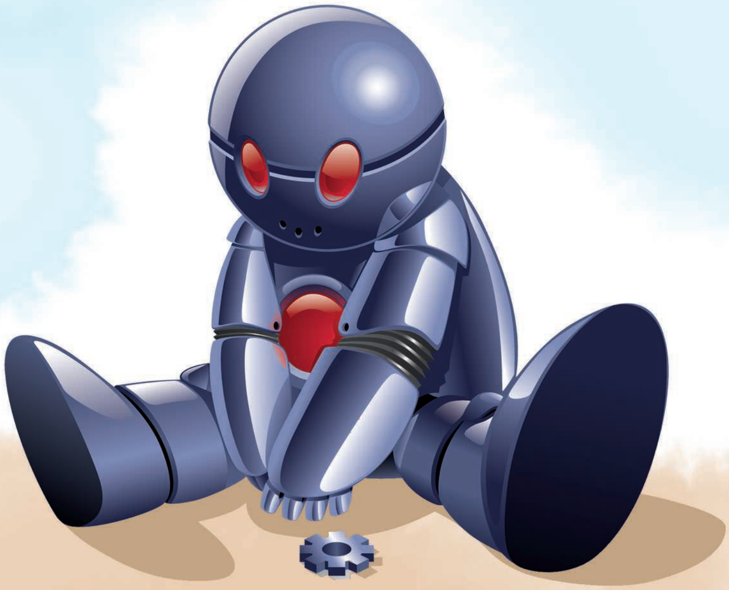

Digital Object Identifier 10.1109/MRA.2019.2943846
Date of current version: 11 November 2019

1070-9932/19©2019IEEE

are accelerating the diffusion of robots in real environments. The first factor is the success of Soft Robotics. Technologies such as series-elastic actuation, variable impedance, and teleimpedance controllers allow machines to interact safely and effectively with humans and the environment. The second factor is the commoditization of hardware and software technologies that, until recently, were relegated to very specialized engineering fields, e.g., nuclear, military, and aerospace. Examples of these technologies include virtual-reality (VR) headsets, integrated inertial navigation units, high-bandwidth and low-latency networking, and, in general, affordable computational power and reliable sensing. The third factor is the growing interest of large companies and funding agencies, which is fostering novel humanoid robotics and teleoperation developments through science competitions and the awarding of prizes. Two popular examples are the 2015 DARPA Robotics Challenge (US$8 million prize) [28] and the recent All Nippon Airways Avatar XPRIZE (XP) (US$10 million prize) [29], "a four-year global competition focused on accelerating the integration of several emerging and exponential technologies into a multipurpose avatar system that will enable us to see, hear, touch, and interact with physical environments and other people through an integrated robotic device" [30]. The focus of the latter includes the domains of health care, services, inspection, and maintenance and demonstrates the importance of physical-interaction capabilities, sensing integration, and user friendliness.

Inspired by these challenges and perspectives, and leveraging our previous experiences and contributions [4], [7], in this article, we present ALTER-EGO. As shown in Figure 1, the robot is a robust and versatile mobile system with a functional anthropomorphic upper body. To operate in different working scenarios and safely perform physical human–robot interactions, ALTER-EGO is powered by variable-stiffness actuators (VSAs), which exhibit a stiffness behavior similar to that of human muscles [8]. Each arm mounts an anthropomorphic, synergistic artificial hand inspired by human motor synergies [7]. The upper body is mounted on a two-wheel, self-balancing mobile base that minimizes the robot's footprint and increases agility. The system is equipped with sensors and computational systems that allow the robot to work autonomously. Moreover, ALTER-EGO can also be used in teleoperation mode from a pilot station mainly composed of lightweight and wearable interfaces. Featuring an immersive control mode, the system can use teleimpedance control [9] to pair the pilot's actions with the robot's mechanical behavior, not only in terms of movements but also in terms of intended interactions behavior.

Most of the hardware and software technologies adopted, developed, and explicitly designed for ALTER-EGO are distributed under an open source framework and are available on the Natural Machine Motion Initiative (NMMI) website [31]. To the best of our knowledge, this is the first time that variable-stiffness technology has been built into an anthropomorphic platform with mobility capabilities and different control modalities ranging from autonomous to teleoperation.

Requirements Analysis

The design requirements of a robot used for assisting with the general activities of daily living differ substantially from those employed for industrial or specialized machines. The tasks required by the XP competition (see Table 1) can be used to distill a set of functional specifications [32] to motivate and guide the design of ALTER-EGO. Note that it is outside the scope of this article to propose a deterministic approach to the definition of robot requirements and specifications or to propose a robot that perfectly fits all these requirements.

ALTER-EGO is powered by variable-stiffness actuators, which exhibit a stiffness behavior similar to that of human muscles.

Manipulation

Half of all the 28 tasks require manipulation and nearly all require physical interaction. Furthermore, the simultaneous presence of tasks 1) where the robot must push large, heavy objects, 2) where finesse and precision are important, and 3) where interaction force control is mandatory (e.g., because of safety) suggests impedance control in the robot arms.

Locomotion

Only three locomotion tasks strictly require the use of legs, making wheels a feasible, yet suboptimal, choice. Nonetheless,

Figure 1. ALTER-EGO: a soft, dual-arm mobile platform equipped with variable-stiffness actuation units and soft, underactuated hands.

Table 1. The tasks and subtasks of the XP competition. (Source: [30]; used with permission.)

			Vision		Hear	Speak	TS	FS		Locomotion		Manipulation	PI	Operation Mode		
	Task Number	Task	First Person	Third Person	–	–	–	Arm	Grasp	Wheels	Legs	–	–	IT	NIT	Autonomous Mode
Scenario 1	X1	Greet your relative in an assisted living facility.	✓	–	–	✓	–	–	–	✓	–	–	–	✓	✓	✓
	X2	Administer morning medications (pills and liquid).	✓	✓	–	✓	✓	✓	✓	✓	–	✓	✓	✓	–	–
	X3	Push a wheelchair 5 m up a ramp to a room.	✓	✓	–	–	–	✓	–	✓	–	–	✓	✓	✓	✓
	X4	Discuss with the staff the daily activities available.	✓	–	✓	✓	–	–	–	✓	–	–	–	✓	✓	–
	X5	Identify a board game such as chess, or retrieve it from a box on a shelf. Then, pick it up, carry it to a table, and set it up for play.	✓	✓	–	–	✓	✓	✓	✓	–	✓	✓	✓	–	–
	X6	Listen to a visiting doctor’s announcement about checkups.	✓	–	✓	–	–	–	–	–	–	–	–	✓	✓	–
	X7	Push your relative 5 m to the doctor’s station.	✓	✓	–	–	–	✓	–	✓	–	–	✓	✓	✓	✓
	X8	Read the written checkup report aloud and sign it.	✓	–	–	✓	✓	✓	✓	✓	–	–	✓	✓	–	–
	X9	Push the relative back down the ramp to his or her original location.	✓	✓	–	–	–	✓	–	✓	–	–	✓	✓	✓	✓
	X10	Take a blanket from a wheelchair, fold it, and put it on a shelf.	✓	–	–	–	✓	–	–	✓	–	✓		✓	–	–
Scenario 2	X11	Use a shovel to load 20 kg of debris into a wheelbarrow.	✓	✓	–	–	–	✓	–	✓	–	–	✓	✓	–	–
	X12	Push the wheelbarrow 10 m to a loading area.	✓	–	–	–	✓	✓	–	✓	–	–		✓	✓	✓
	X13	Use the shovel to unload the wheelbarrow.	✓	✓	–	–	–	✓	–	✓	–	–	✓	✓	✓	✓
	X14	Return the wheelbarrow to its original location, and listen for a call for help.	–	✓	✓	–	–	–	–	✓	–	–	–	–	✓	✓
	X15	Locate the source of the call for help.	✓	✓	✓	–	–	–	–	–	–	–	–	–	–	✓
	X16	Walk forward on a rough dirt surface toward that location.	✓	✓	–	–	–	–	–	–	✓	–	✓	–	✓	✓
	X17	Pick up a coiled rope with a weighted end.	✓	–	–	–	✓	–	–	✓	–	✓	–	✓	✓	✓
	X18	Throw the weighted end of the rope toward the sound of the call for help.	✓	✓	✓	–	–	–	–	✓	–	✓	–	–	–	✓
	X19	Turn your head and call loudly for assistance.	✓	–	–	✓	–	–	–	–	–	–	–	✓	✓	–
	X20	Hand the unweighted end of the rope to an assistant.	✓	✓	–	–	–	✓	–	✓	–	✓	✓	✓	✓	✓
	X21	Locate a set of instructions and read them aloud.	✓	–	–	✓	–	–	–	–	–	–	–	✓	✓	–

Scenario 3	X22	Pour a specified quantity of fluid from one beaker to another.	✓	–	–	–	✓	✓	✓	✓	–	✓	✓	✓	–	–
	X23	Use a scoop to collect a specified sample of powder.	✓	–	–	–	✓	✓	–	✓	–	✓		✓	✓	✓
	X24	Unroll a plan on a flat table and place weights on its corners.	✓	✓	–	–	✓	✓	–	✓	–	✓	✓	✓	–	–
	X25	Using a protractor, straightedge, and mechanical pencil, draw two lines on the plan that intersect at 45°.	✓	–	–	–	✓	✓	✓	✓	–	✓	✓	✓	–	–
	X26	Identify the broken plug-in components on an electrical panel.	✓	–	–	–	✓	✓	✓	✓	–	✓	–	✓	–	✓
	X27	Walk 6 m to a workbench and solder a wire onto it.	✓	–	–	–	✓	✓	✓	✓	–	✓	–	✓	–	✓
	X28	Return to the control panel and replace the component.	✓	–	–	–	✓	✓	✓	✓	–	✓	–	✓	–	✓
	–	The total XPRIZE tasks.	28	13	5	6	13	17	8	23	1	13	14	24	15	16

TS: touch sensing; FS: force sensing; PI: physical interaction; IT: immersive teleoperation; NIT: nonimmersive teleoperation.

it is important to note these requirements in terms of agility (thus, its small footprint).

Intelligence

The combined requirements of all the tasks in terms of intelligence concede the unfeasibility of either a fully autonomous or fully teleoperated solution and favor a shared-autonomy approach. Indeed, although the performance of some tasks could benefit from an immersive teleoperation that enhances the pilot's sense of presence, other tasks may prefer console-based teleoperation, which minimizes fatigue, while still others favor autonomous operation.

Sensing

Vision is the most important sensory system and is required for nearly every task. Nevertheless, the possibility to abstract from the subjective viewpoint (the "eyes" of the robot) a third-person point of view can benefit the operator's scene awareness in 13 of 28 tasks. Hearing (five/28 tasks) and speaking (6/28) capabilities play a fundamental role in inspection and social-interaction activities. All the tasks that involve physical interaction require touch sensing (13/28) or force sensing (17/28). Accordingly, this also raises the issue of delivering touch and force feedback to the operator's senses. It is outside the scope of this article to discuss all of these technologies in detail. The reader is encouraged to refer to [11] for a review of the technologies and to the "Pilot Interface" section for a description of the solutions integrated into the proposed system.

Pilot Station

The XP competition also explicitly addresses the fundamental aspects of the usability and intuitiveness of control interfaces for nontrained users. These requirements should reflect several aspects of the robot's design, thus paving the way to another relevant consideration, i.e., that the robotic system is not constituted solely by the robot itself; rather, it is combined and integrated with the infrastructure that must be used to effectively operate it—the pilot station. This underlines the relevance of aspects such as the graphical user interface and its software capabilities, the ergonomics of the input devices, the time needed to set up the system, and the overall weight of the wearable devices used by the operator (especially in immersive teleoperated modalities).

ALTER-EGO

Figure 2(a) presents a few kinematic and mechatronic details of ALTER-EGO. The mobile platform has two independent wheels actuated by two dc motors. The upper body has 5 degrees of freedom (DoF) for each of the two arms and integrates a robotic head mounted on a 2-DoF neck, which allows the head to pan and tilt, as shown in Figure 2(a) and (b). The neck is mounted on the trunk. All of the upper body's DOF are actuated by VSA units that enable safe, physical interaction with the environment as well as people. The presence of VSA units also increases the robustness of the system both in terms of both control (because the soft behavior mitigates passively external disturbances, e.g., from balance control) and mechanical failures (e.g., during a fall). Moreover, the adoption of the same actuation units in all of the robot's joints yields a simple modular architecture (i.e., all of the joints are assembled with the same interconnection flanges), which facilitates reconfiguration and parts substitution (e.g., in the event of a failure).

Two soft, anthropomorphic hands complete the robot's upper body design.

The robot's footprint clearance is 500-mm wide and 260-mm deep, while the robot's height is 1,000 mm. The robot weighs approximately 21 kg, and its two-handed payload is 3 Kg, yielding a 0.143 weight-to-payload ratio. Its average speed is 0.25 m/s. The autonomy of the robot, in combined usage condition, ranges between 4 and 6 h. The following subsections briefly describe the manipulation, locomotion, and sensing subsystems composing ALTER-EGO. Note that 1) all details about the building blocks forming ALTER-EGO and 2) all instruction on how to assemble, run, and operate the system can be downloaded from the NMMI website and GitHub webpage [32] (see also [7]).

Locomotion

The robot's lower body is composed of a rigid frame connecting the upper body to a two-wheeled mobile base, as displayed in Figure 2(a) and (b). Although most of the robots used in structured scenarios have at least three wheels to help avoid stability problems, this often leads to the introduction of tradeoffs between mobility and agility, i.e., the adoption of small wheels to minimize its footprint, which eliminates the system's ability to deal with obstacles. For this reason, we chose to equip ALTER-EGO with only two wheels to avoid the tradeoffs discussed in [12] and [13]. Each wheel has a diameter of 260 mm; is equipped with a low-profile, off-road tire; and is powered by a 12-V Maxon dc motor (DCX 22L) in combination with a Harmonic Drive gearbox (160:1). The lower body of the robot [see Figure 2(b)] includes a nine-axis inertial measurement unit (IMU) (MPU-9250 TDK InvenSense) between the two wheels, to estimate the pitch angle, and two magnetic encoders (AS5045 Austrian MicroSystems), to measure wheel rotation. Additionally, two Sharp infrared GP2Y0A02YK0F sensors are integrated into the base to prevent collision with low-clearance obstacles.

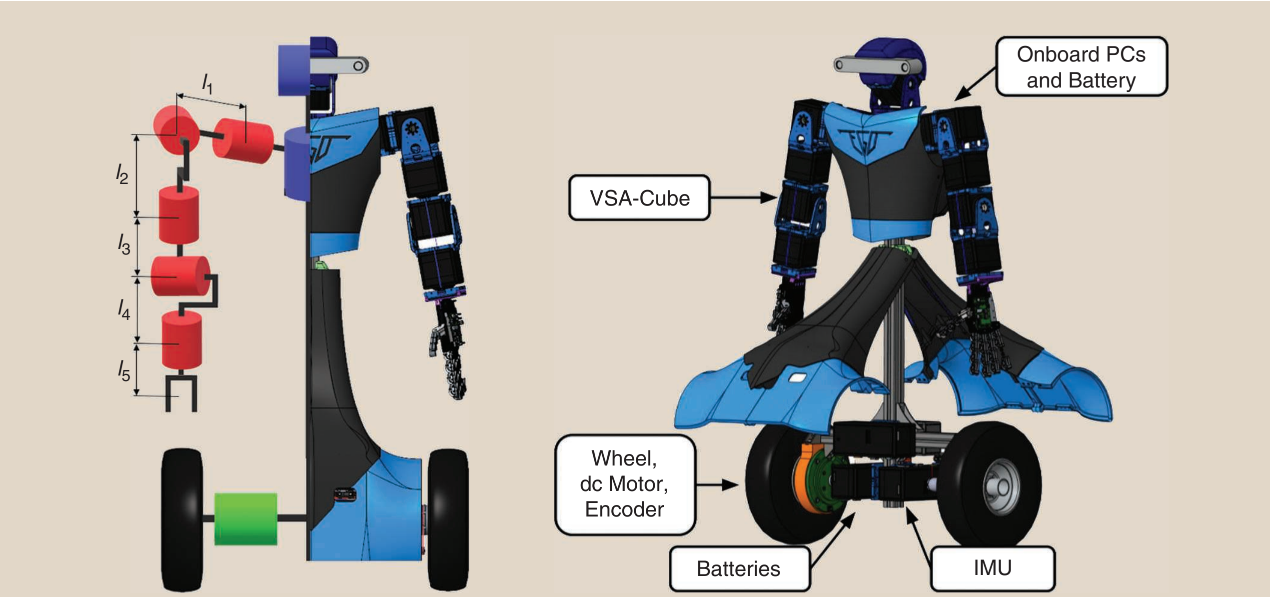

(a) (b)

Right Arm				
Link	a_i	α_i	d_i	θ_i
1	ϕ	$\pi/2$	l_1	θ_1
2	ϕ	$-\pi/2$	ϕ	$\theta_2 + \pi/2$
3	ϕ	$-\pi/2$	$l_2 + l_3$	$\theta_3 - \pi/2$
4	ϕ	$\pi/2$	ϕ	θ_4
5	ϕ	$-\pi/2$	$l_4 + l_5$	θ_5

(c)

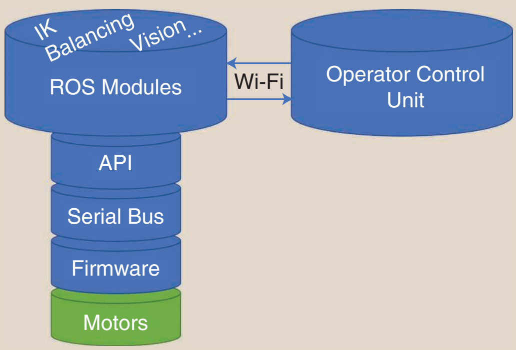

(d)

Figure 2. (a) and (b) The mechatronic architecture of ALTER-EGO. (c) and (d) The Denavit–Hartenberg parameters of the arms and the overall software architecture. l_i represents the length of ith link, and a_i, α_i, d_i, and θ_i are the Denavit–Hartenberg parameters of the ith link [10]. IMU: inertial measurement unit; ROS: Robot Operating System; API: application programming interface; IK: inverse kinematics. (Source: [30]; used with permission.)

Independently controlling the two wheels allows the system to move forward and backward and to turn in place. Furthermore, the possibility of the robot adapting its pitch angle to the dynamical conditions improves its execution of push/pull tasks as well as its tackling of slopes (see the "Experiments and Discussion" section for more details).

Note that this solution is not devoid of drawbacks; indeed, the platform requires active balance stabilization, which may incur instability issues and increase its energy consumption. Additionally, balance control may also have consequences on the manipulation capabilities of the system. Accordingly, changes to the robot's center of mass (CoM) can affect the Cartesian position and orientation of the head and end effectors. These effects can have negative consequences (e.g., in a teleoperation setting; see also the "Operating Modes" section) and make manipulation more difficult unless 1) careful control ensures that the end effectors are not affected by these oscillations or 2) the pilot actively manages such changes. See the "Experiments and Discussions" section for more details.

In the "Control" section, we describe the stabilization controls implemented in the robot; in the "Experiments and Discussions" section, we demonstrate how the robot acts in the event of accidental impacts and how it is capable of stably interacting with its environment. The complete solution of such problems requires a deeper investigation, including the introduction of improved-control algorithms, mechanical safety systems, or possibly both. In this regard, with ALTER-EGO, it is possible to activate a whole-body balancing controller (as opposed to the more conventional linear quadratic regulator (LQR) control, see the "Control" section) that takes full advantage of the system's dynamics, e.g., the arms, to improve balancing performance (see [14]).

Manipulation

A revised release of the University of Pisa/Italian Institute of Technology's SoftHand (SH) [7] was specifically designed for ALTER-EGO. SH's purpose is to match the robot's payload and dimensions (i.e., a weight of 0.29 kg and a length of 130 mm). The SH is a heavily underactuated anthropomorphic hand (19 DoF actuated by a single motor), capable of self-adapting its grasp to objects of different shape, size, and weight and interacting with people and its environment safely and effectively.

The main actuators of ALTER-EGO's arms and neck are 12-qb move units, which are modular VSAs derived from the VSA-CUBE design [7], that implement an agonistic-antagonistic principle using two motors connected to the output shaft through a nonlinear elastic transmission. Each module can mechanically change its output shaft position and mechanically set a given output shaft-stiffness profile.

The anthropomorphic structure of the upper body is achieved by connecting both arms to a frame, which, in turn, is mounted on the mobile base [Figure 2(a) and (b)]. Each arm presents a relative angle with respect to the frame so as to maximize the common manipulation in the workspace, a solution commonly used in other bimanual systems (e.g., [4]). Each arm has 5 DoF; for this reason, the robot may incur unreachable configurations and singularities, especially when teleoperated. Such kinematics are the result of a tradeoff between weight, complexity, arm length, and the actuators' maximum payload. Note that different, more anthropomorphic shoulder configurations that include increased payload capabilities are currently under investigation (refer to [15] for more details).

The platform requires active balance stabilization, which may incur instability issues and increase its energy consumption.

Assuming the preferred end-effector pose (position and orientation), the required joint positions of each arm are computed via a closed-loop, inverse-kinematics (IK) algorithm with damped pseudoinverse [10]. The orientation of the pilot's head is mapped directly to the corresponding Euler angles (pitch and yaw) of the robot's neck, as depicted in Figure 3(a). For each qb move of the upper body, a position/stiffness control is used. Given the elastic nature of VSA, to control the position of the robot arms in feedforward mode without a steady-state error, it is necessary to compute both the desired actuator position and the expected load torque, τ, to compensate for the expected elastic deflection, δ. The vector τ can be easily extracted by the robot dynamics as

$$\tau = B(q)\ddot{q} + C(q, \dot{q})\dot{q} + G(q) - J^T f_e, \tag{1}$$

while the expected deflection can be reconstructed by inverting the elastic model of the qb move,

$$\tau = k_1 \sinh(a_1(q - \theta_1)) + k_2 \sinh(a_2(q - \theta_2)), \tag{2}$$

where (k_1, k_2, a_1, and a_2) represent the model parameters reported in the data sheet available on the NMMI website, q is the link position, and (θ_1 and θ_2) are the positions of the two motors. Because $k_1 \simeq k_2 = k$ and $a_1 \simeq a_2 = a$, it is possible to write τ as

$$\tau = 2k \cosh(a\theta_{\text{pre}}) \sinh(a(q - \theta_{\text{eq}})), \tag{3}$$

where

$$\delta = q - \theta_{\text{eq}}, \theta_{\text{pre}} = \frac{\theta_1 - \theta_2}{2}, \theta_{\text{eq}} = \frac{\theta_1 + \theta_2}{2} \tag{4}$$

are the deflection, stiffness regulation, and equilibrium angles, respectively. Given a desired θ_{pre} and q, it is possible to reconstruct from (3) the expected deflection $\delta = \delta(q, \theta_{\text{pre}})$; thus, the expected motor trajectory is $\theta_{\text{eq}} = q + \delta(q, \theta_{\text{pre}})$. Figure 3(b) shows the adopted compensation scheme, where, for simplicity, $\tau \approx G(q)$.

Control

In a simplified model, the state-space of the lower body subsystem has three generalized coordinates (θ, ψ, and ϕ), which describe the semisum of the wheel angles and the robot's yaw and tilt angles, respectively. Figure 3(a) expresses the balance control scheme, with $u = [u_1 \; u_2]$ representing the torque control for the two wheels, and $e = r - y$ being the error between the current y and required r robot states. The anticipated state can also be modified by the operator using the available teleoperation devices (see the "Operating Modes" section). A classical LQR method can be applied to stabilize the wheel base (as in [16] and [17]), which can be simply designed but does not take advantage of the arms' fast-balancing motions. This method is suitable when arms are not available to balance (e.g., because they are used in other tasks) and provides good balancing performance, as presented in the "Experiments and Discussion" section.

To improve independent LQR control performance, in [14], we developed a new whole-body dynamic control system that computes the joint actuation torques τ, given a preferred joint-space motion to track. To achieve this, a computed torque-control law in the quasi-velocity vector was developed, starting from the underactuated and kinematically constrained model of ALTER-EGO. Note that the model discussed in [14] does not take into account the variable stiffness of the robot's upper body explicitly, which remains an open subject of research.

The idea of [14] follows in brief. Let q be the generalized coordinates of the robot, n the number of DOF, n_{fb} the number of independent variables needed to describe the floating base motion, and n_c the number of constraints acting on the robot, e.g., due to base kinematics. Then, let $\nu \in \mathbb{R}^{n+n_{fb}-n_c}$ be the quasi-velocity vector so that $\dot{q} = S(q)\nu$. Consider the error dynamics

$$\dot{\nu}^d - \dot{\nu} + K_d(\nu^d - \nu) + K_p \int_0^t (\nu^d - \nu) = 0, \qquad (5)$$

where K_p and K_d are positive definite gain matrices and ν^d are the desired quasi-velocities. The resulting

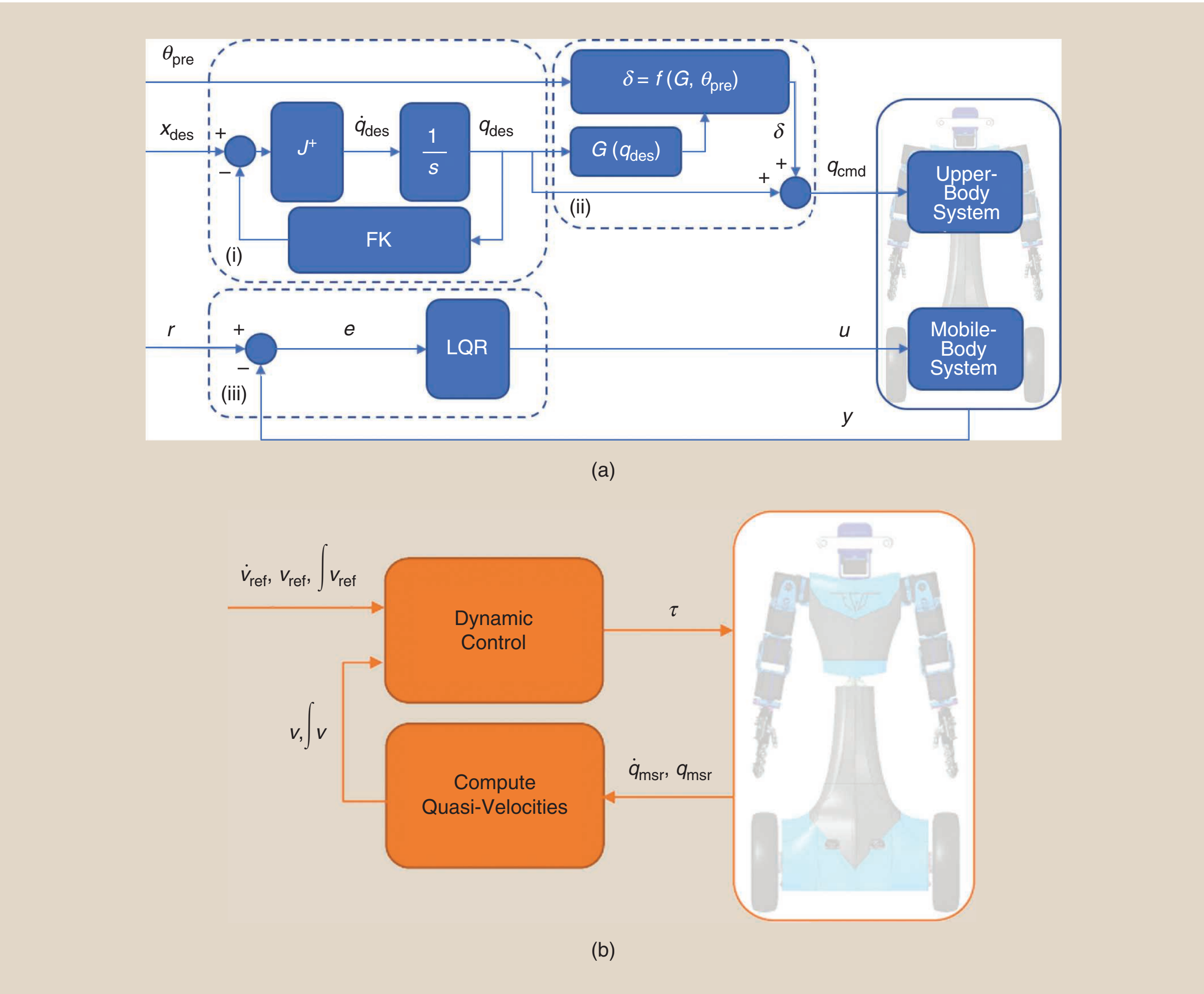

Figure 3. The ALTER-EGO control schema. (a)The full-state feedback control system obtained with LQR. (b) The whole-body control schema. FK: forward kinematics.

generalized torques are computed as a function of the quasi-velocities vector:

$$\tilde{\tau} = \tilde{M}\Big(\dot{\nu}^d + K_d(\nu^d - \nu) + K_p \int_0^t (\nu^d - \nu)\Big) + \tilde{c}, \quad (6)$$

where $\tilde{c} = S^T(q)(M(q)\dot{S}(q,\dot{q})\nu + C(q,\dot{q})S(q)\nu + G(q))$ and $\tilde{M} = S^T(q)\,M(q)S(q)$. This ensures that the resulting generalized torques are compatible with the constraints by design. We show in [14] that the actual joint torques τ can be obtained from (6) to achieve a whole-body control method. The method was tested in several experiments to stabilize the robot around an equilibrium position in the presence of static and dynamic disturbances [see Figure 4(c) and (d)] as well as in tracking some required motions during the execution of a task that included physical interaction with the environment.

Sensing

The head is equipped with a Stereolabs Zed Camera [33]. This is a passive red-green-blue-depth (RGB-D) camera that can acquire images, videos, and a depth point cloud of the scene. Images can be streamed to either the pilot station monitor or to the VR headset when the robot is used in teleoperation mode (see the "Operating Modes" section). ALTER-EGO is equipped with a set of basic vision tools that enable it to recognize objects and markers. A wrapper is available, making the Zed stereo camera usable in the Robot Operating System (ROS) environment by providing access to stereo images, the depth map, the 3D point cloud, and 6-DoF tracking. Currently, several software systems exploit state-of-the-art object-detection algorithms. For this purpose, Detectron [34] has been used on ALTER-EGO. The head architecture is completed by a 10-W speaker and a multidirectional, six-channel microphone.

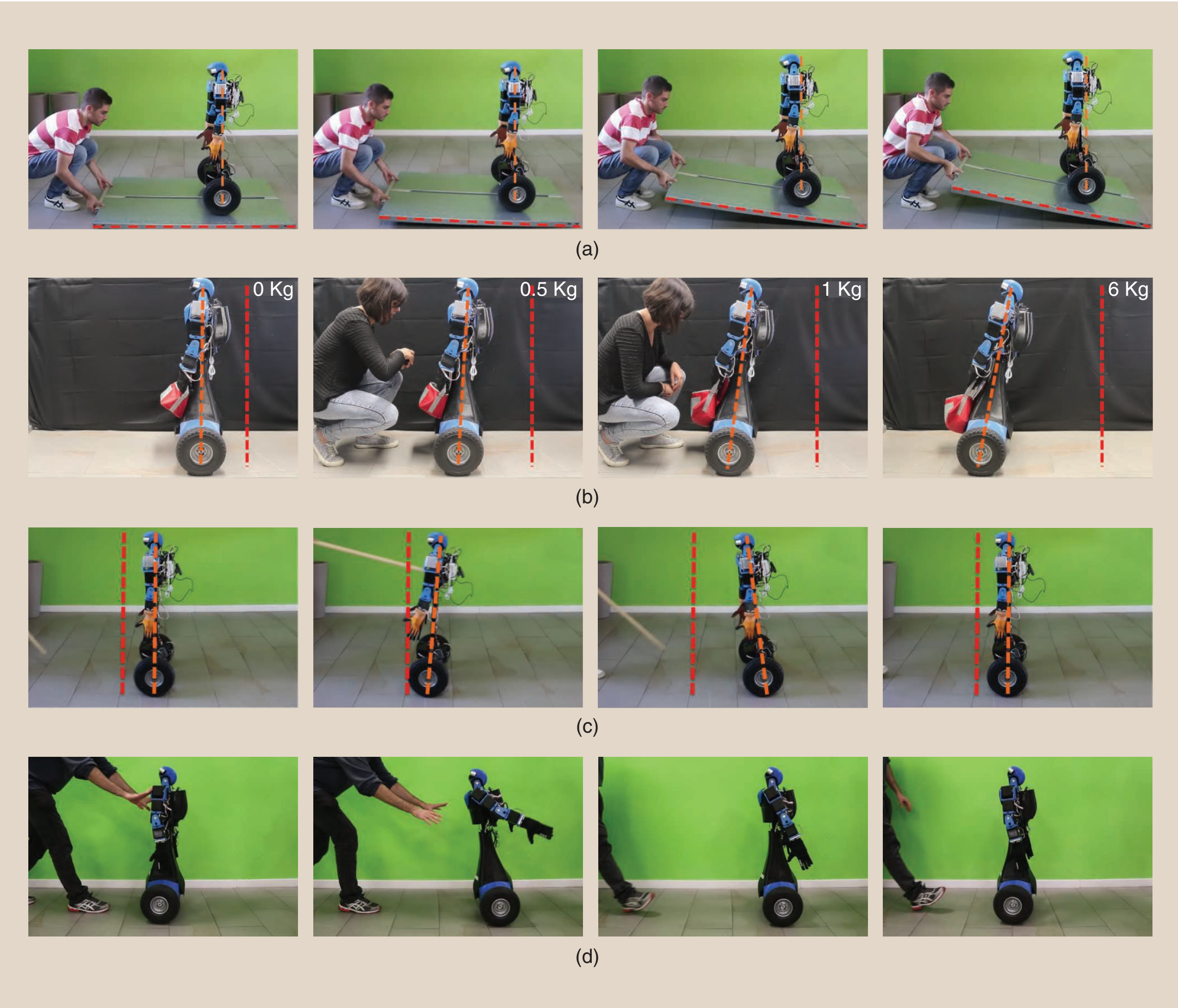

Figure 4. (a) The robot balancing at different slope angles. (b) The robot balancing in the presence of static disturbances. (c) The LQR control algorithm; the robot balancing in the presence of external impulsive disturbances. (d) The whole-body control algorithm; the robot balancing in the presence of dynamic disturbances.

Both hands are equipped with position and current sensors on their motors to reconstruct the applied grasp force. Additionally, the hands' fingertips can be conveniently equipped with IMUs to allow for the estimation of contact events and surface roughness, as described in [18]. Each actuation module is equipped with three position sensors (on the two prime movers and on the output shaft) to measure the spring deflection. This measurement can be used to estimate the torque applied by each motor and, in turn, to estimate the external wrenches applied to the end effectors, using the least-square approach explained in [19].

Mechatronics, Software, and Communication Architecture

ALTER-EGO is equipped with a computational unit (NUC i5 compact computer) for managing the control architecture, vision streaming, and compression algorithms. The low-level communication layer between the actuation units, wheels, sensors, and end effectors is based on an RS485 protocol (2 Mb/s).

The robot is equipped with two 24-V batteries that have a total capacity of 48,000 mAh and a peak current of 100 A. A dedicated 12-V battery with a total capacity of 30,000 mAh is used to supply the computational units.

The ALTER-EGO software architecture is organized into four layers, as displayed in Figure 2(d). The first layer is constituted by the firmware running in each board used to control the joints, end effectors, motor wheels, and sensors. A second layer, also embedded in the electronic boards, manages the communication bus among the different devices that constitute the robot's hardware. A third software layer (i.e., an application programming interface) supports the communication between the second layer and the ROS modules. Each ROS module manages the nodes used for the base motion, balancing, arms-IK, feedforward gravity compensation, end-effector wrench estimation, localization, mapping, navigation, and vision. Finally, a fourth layer is used to communicate with the pilot station and manages the robot in both autonomous and teleoperated modes.

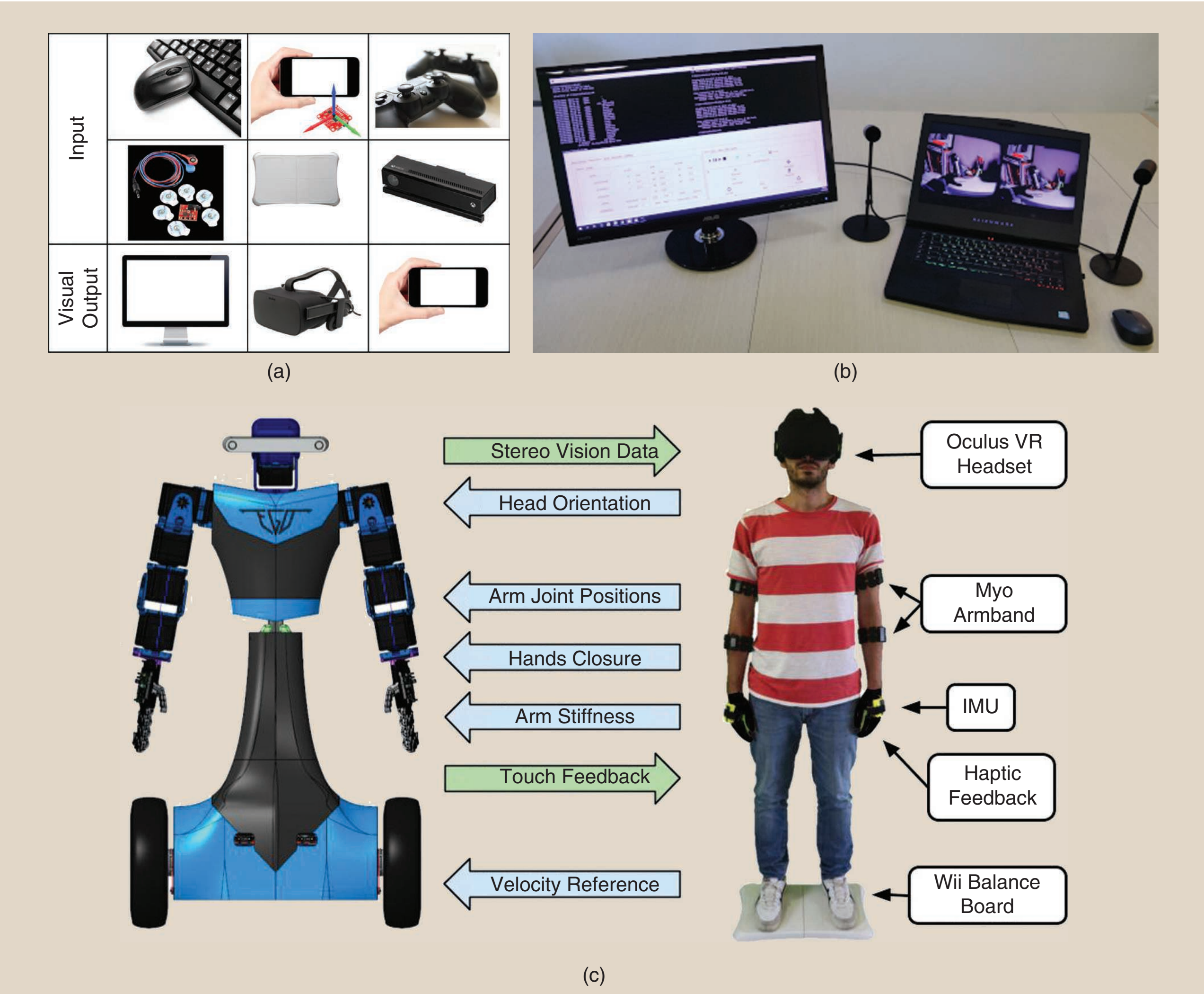

Figure 5. (a) ALTER-EGO's input and output interfaces. (b) The pilot station used for autonomous and teleoperation mode and (c) the pilot station used for immersive teleoperation mode.

A dedicated communication framework enables the exchange of data between the robot and pilot station. A 5-GHz wireless connection allows for bilateral communication with the pilot station for the streaming of control (e.g., sensors measurements and references positions) and vision data. An ROS communication framework is used to send commands to the robot and receive data from it. A dedicated User Datagram Protocol connection was developed to foster video data exchanges between the robot and pilot station (see the "Operating Modes" section). At a frequency of 100 Hz, the pilot station sends the robot references of head orientation, arm joint position and stiffness, hands closure, and velocity vector for the mobile base (Figure 5). The robot sends back a stream of images at a frequency of nearly 25 Hz; they are, however, limited by capturing and processing delays. The measured average ping time between the pilot station and the robot is 15 ms, while the average bandwidth used for both motion commands and image streaming was measured; accordingly, bandwidths of 1 Mb/s and 18 Mb/s, respectively, were used. In some experiments, Internet infrastructures were employed to connect the pilot station to the robot operation site, where it is completed by 5-GHz Wi-Fi.

Operating Modes

Autonomous Mode

ALTER-EGO has two main operation modalities. In autonomous mode, ALTER-EGO can be used in a completely independent fashion, leveraging core functionalities embedded in its local computational unit. For autonomous navigation, simultaneous localization and mapping (SLAM) algorithms are used. More specifically, an RGB-D graph SLAM approach based on a global Bayesian loop-closure detector is employed, i.e., Real-Time Appearance-Based Mapping (RTAB-MAP) [20]. Although the use of RTAB-MAP allows ALTER-EGO to be localized accurately, camera occlusion and slow update rate (10 Hz) impede robot localization in some cases. To solve this problem, a particle filter [21] is integrated into the system. Ultimately, the wheel velocity (measured by encoders) and visual odometry (obtained by RTAB-MAP) were used for prediction and correction phases, respectively. Particle filters are employed to ascertain the robot's current position and orientation. This information is used as feedback for waypoint-based navigation. For this purpose, the pure pursuit method [22] was applied to ALTER-EGO. ALTER-EGO is also equipped with autonomous grasping and manipulation capabilities, which make it capable of grasping objects with two hands, using both vision and

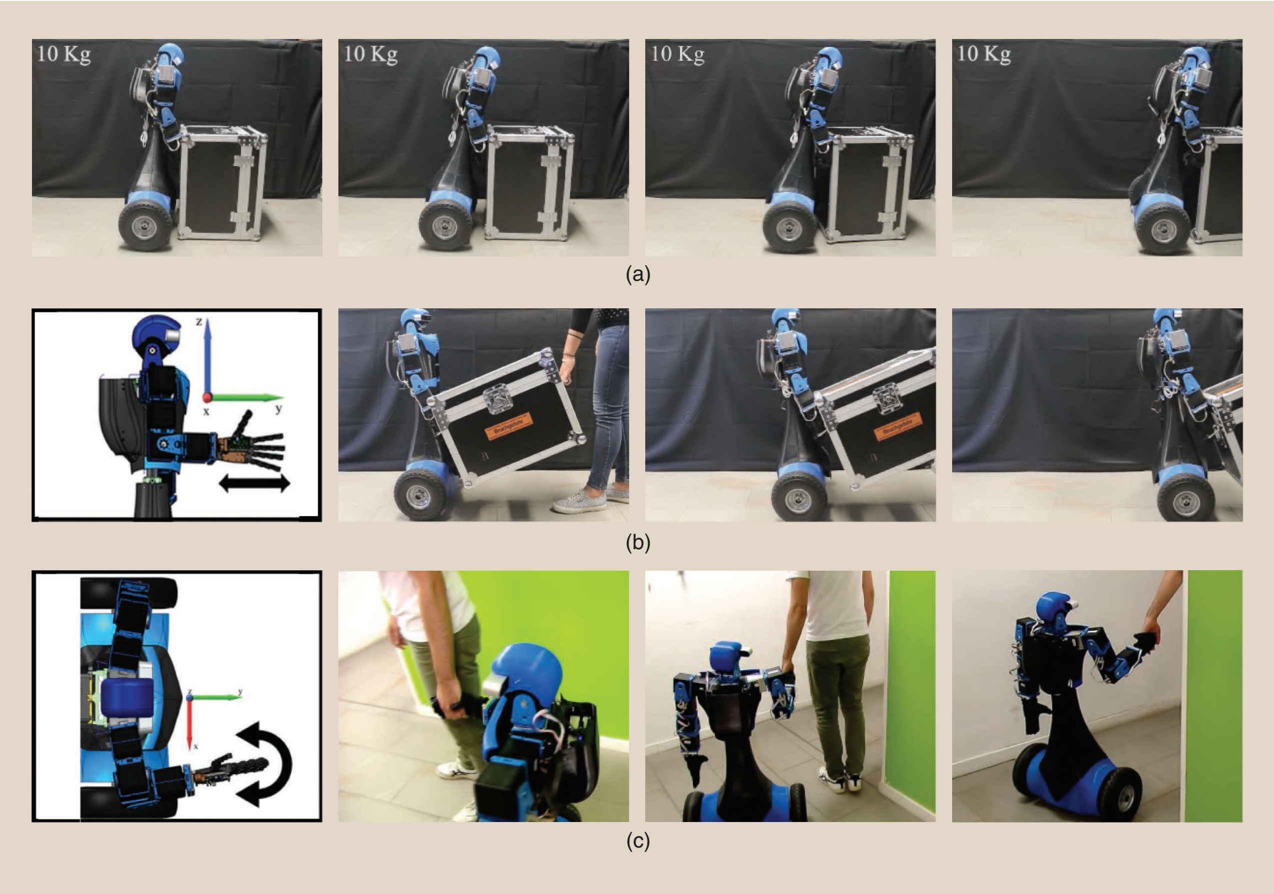

Figure 6. ALTER-EGO's autonomous actions. ALTER-EGO (a) pushing a heavy box (10 kg), (b) carrying a heavy box in collaboration mode with a human, and (c) following a human operator.

end-effector wrench estimation. An Aruco [35] ROS package was utilized to determine an object's position.

ALTER-EGO embeds an autonomous modality that enables the execution of collaborative tasks together with humans. In this operational mode, ALTER-EGO executes cooperative manipulation tasks, e.g., handling an object in cooperation with humans or walking hand in hand (Figure 6). To execute these kinds of tasks, an end-effector wrench estimation is used. In particular, the force in y direction and the torque around z direction are used as the desired linear and angular velocity, respectively, to follow the direction imposed by the human [see Figure 6(b) and (c)].

ALTER-EGO can be teleoperated from a console or through an immersive VR setup.

Teleoperation Mode

ALTER-EGO can be teleoperated from a console or through an immersive VR setup. In the latter case, a motion-capture system is needed to map the pilot's body movements to the robot's kinematics. A key feature of the proposed teleoperation framework is its lightweight, reduced encumbrance and ease of wear. In the standard setup, two Myo armbands per arm (one placed on the forearm and one on the upper arm) plus an additional IMU placed on the pilot's hand permit the reconstruction of the Cartesian position and orientation of the pilot's limbs. Let ${}^{i}T_j \in R^{4\times4}$ be the homogenous transformation from joint i to joint j; the homogenous transformation ${}^{S}T_H$ from the shoulder to the hand is given as

$$ {}^{S}T_H = {}^{S}T_E \, {}^{E}T_W \, {}^{W}T_H, \tag{7} $$

where subscripts S, E, W, and H indicate shoulder, elbow, wrist, and hand, respectively. The translation part of every homogenous transformation is known a priori (i.e., length of the arm and forearm, and the distance between the wrist and palm), whereas it is possible to compute ${}^{i}R_j \in R^{3\times3}$ (rotation part of the homogenous transformation ${}^{i}T_j$) by applying a Madgwick filter [23] on the data coming from the IMU placed on the arm and on the hand. The result of (7) is properly scaled to match with the length of the robot's arms and then used as a Cartesian reference for the IK algorithm. This setup allows for controlling the stiffness of the robot arms using the electromyographic data given by the Myo armbands placed on pilot's upper arm, thus implementing teleimpedance control [4]. Hand closure is controlled by a linear combination of electromyographic signals from the Myo armbands placed on the pilot's forearms [7]. In this configuration, a Wii Balance Board [36] is used to control the robot's mobile base by sending velocity references. More specifically, an operator can use his or her own CoM to move the robot forward and back and turn left and right. This configuration is preferable when haptic feedback devices must be used, mainly because it leaves free the operator's hands. In some circumstances, a simplified version of the capture system can be used simply by relying on the sensors provided by the VR system adopted (e.g., Oculus Rift).

Pilot Interface

ALTER-EGO has a modular pilot interface that can be shaped according to different purposes and operation modalities. The key elements are input, visual, and haptic feedback interfaces. All of these elements can be selected and switched

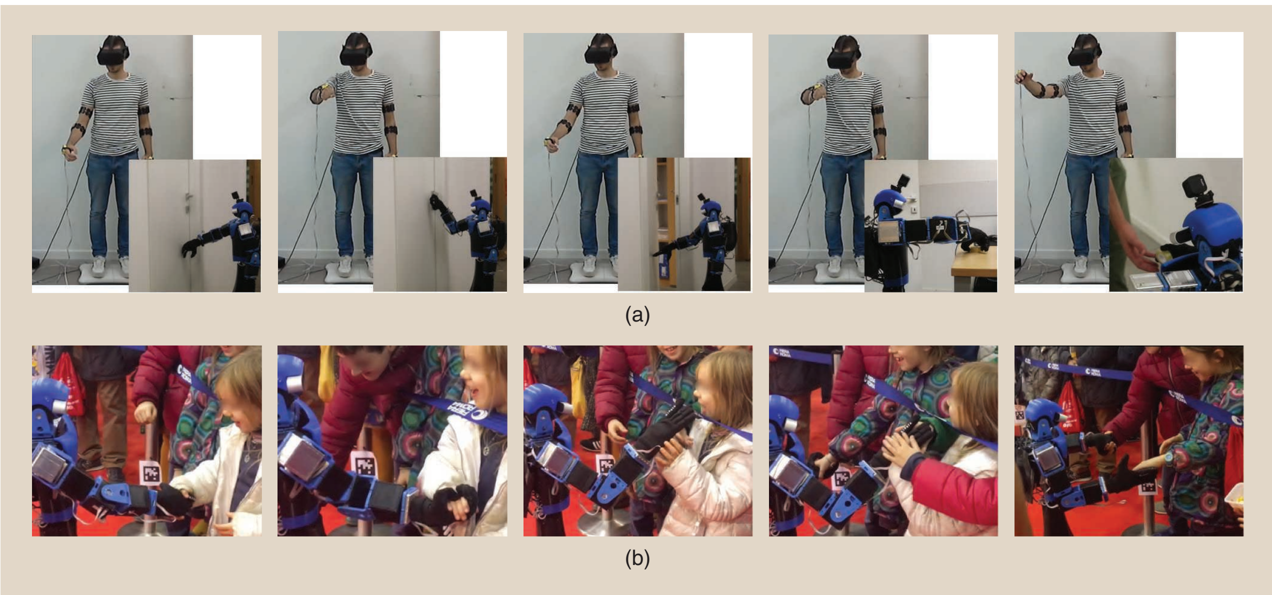

Figure 7. (a) ALTER-EGO opens a door and grasps an object. (b) ALTER-EGO physically interacts with children. (Source: MakerFair; used with permission.)

during a session. A description of each subsystem of the pilot interface is reported in the following sections.

Computational and Communication Console

ALTER-EGO's pilot station comprises one laptop used to manage, monitor, and command the robot together with the different interfaces. The same laptop is operated to handle the vision workload to manage 3D and 2D visualization, the VR framework, and vision algorithms. The pilot console is also equipped with a dedicated wireless router.

Visual Interfaces

ALTER-EGO has two main visual interfaces: a standard screen visualization and immersive, first-person VR visualization. With the first option, it is possible to visualize all of the robot's parameters on a screen together with the visual streaming coming from RGB cameras. Likewise, using the support of ROS 3D visualizers (see the "ALTER-EGO" section), it is possible to produce a 3D reconstruction of the environment together with the 3D pose reconstruction of the robot. As a second option, ALTER-EGO also integrates the use of a VR headset, such as those used for Oculus Rift. In this configuration, an immersive visual representation of the world is possible.

Input Interfaces

Several input devices can be used to acquire or compute references for the robot, for both the locomotion and manipulation subsystems. Common joystick/joypad, keyboards, and mouses move the robot's mobile base and arms and buttons activate hands or start predefined functions. Currently, a balance board (WII) is employed to control the forward/backward and turning movements of the mobile base. Wearable devices such as the Myo armband (a nine-axis IMU, plus eight-channel surface electromyography sensors) are used to control activation of the robot's hands, manage the impedance of the actuation units, and perform motion capture of the pilot's movements in teleoperation mode (see the "Operating Modes" section). If a VR headset is present, its motion-capture system can be used to control the robot's movements.

Haptic Feedback Interfaces

The ALTER-EGO pilot station was conceived to allow the pilot to use different haptic feedback devices for delivering different haptic stimuli, which can be conveyed on the hands of the pilot or on others parts of his or her body (e.g., the arms). To avoid typical issues related to instability as a result of the adoption of closed-loop controls, ALTER-EGO uses noncollocated feedback systems. Moreover, in most cases, a modality-matching approach is followed [11]. Examples of feedback stimuli developed under the same NMMI framework that can be used in the platform are hand grasp force [24], impacts and surface roughness [18], and hand proprioception [25].

Experiments and Discussion

This section reports on experimental examples to demonstrate the effectiveness of the system's basic capabilities and describe application examples where ALTER-EGO is used in physically simulated and realistic contexts. The pictures and photo sequences referenced in this section are extracted from the video footage linked to this article.

ALTER-EGO's pilot station comprises one laptop used to manage, monitor, and command the robot together with the different interfaces.

Figure 7 shows the robot executing different tasks in different contexts. In Figure 7(a), ALTER-EGO is used in immersive teleoperation modality to open a door, grasp an object, and provide it to a third user. The movements of the robot and the human operator are visible. Figure 7(b) shows ALTER-EGO interacting with children during an exposition (MakerFair in Rome, Italy).

Figure 8 depicts ALTER-EGO operating in a domestic use-case scenario. The actions shown are mostly executed in the immersive teleoperation operating mode and envision a hypothetical user jumping inside the robot at his or her work location and teleporting him or herself home to perform domestic tasks. In Figure 8(a) and (b), the pilot uses the robot to prepare food for a pet and to retrieve a package from a mail carrier, pay for the item, and return to the house. In Figure 8(c), the pilot remotely simulates ALTER-EGO

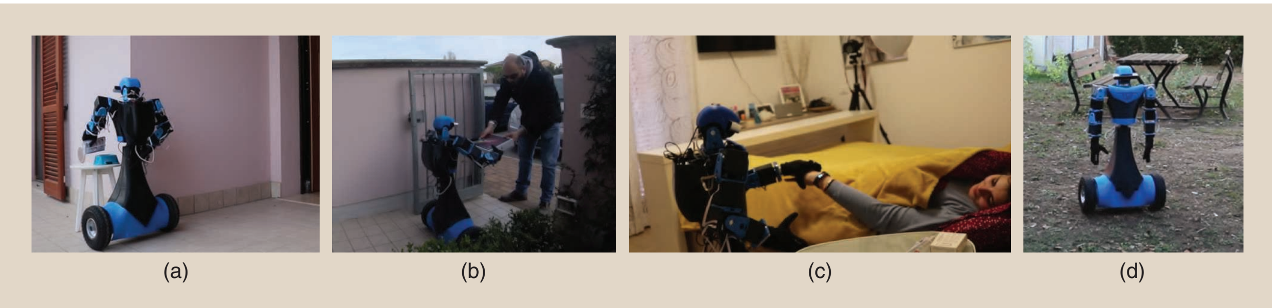

Figure 8. (a) and (b) The robot is teleoperated to prepare food for pets and retrieve a package from a mail carrier. (c) ALTER-EGO assists a pilot's relative. (d) The robot is operated in an outdoor terrain with small rocks, grass roots, and a slight descent.

assisting a relative. In this scenario, ALTER-EGO provided a thermometer and pills to the relative, checked the relative's temperature, offered a blanket, checked the cardiac frequency, and presented food. The experimental activity was performed at two different locations positioned at a distance of 5 km (the pilot station was placed in the engineering building on the campus of the University of Pisa), and the telecommunication framework used an Internet connection with a bandwidth of 48 and 80 Mb/s in download and 48.3 and 18 Mb/s in upload for the pilot station and domestic environment, respectively. The ping was 17 ms. Although not exhaustive, such an experience demonstrates the potential effectiveness of the approach. Finally, Figure 8(d) shows ALTER-EGO moving on an outdoor, uneven terrain characterized by the presence of small rocks, grass roots, and a slight descent.

We would like to point out and discuss a few of the drawbacks experienced while using the proposed platform. The advantages of using an agile, two-wheeled mobile base can be counterbalanced by the instability of the platform. Indeed, this can have critical, even catastrophic effects, e.g., in the case of impacts with the environment during a manipulation task. The CoM variation (e.g., movements of the arms or variation of payload) is used to update the feedforward action (preferred pitch angle) to stabilize the robot. With the LQR control approach, the perturbation on the end effector's desired pose (due to the stabilizing controller) can be corrected and compensated for only by the pilot, who must close the external control loop through the vision feedback provided by the VR headset. We acknowledge that this approach is a rather simplistic solution to the problem, and better solutions could certainly be devised.

Nevertheless, in the videos, the pilot accomplishes the tasks notwithstanding the disturbances. In our experience, such phenomena are well addressed when the robot is teleoperated in an immersive mode because the pilot–robot interaction is intuitive and the pilot has an idea of what is happening in the scene. Although we have only episodic data, one could venture to say that human pilots exploit their own instinctive ability to compensate for stabilization and manipulation interactions. For this reason, we also introduced the whole-body balancing control method described in the "Control" section. Using this controller, balancing performance improves; however, a more in-depth investigation is needed to better evaluate its performance during manipulation tasks. Note that other possible approaches to the autonomous decoupling of manipulation and stabilization include the introduction of active counterbalance mass, as seen, e.g., in recent Boston Dynamics footage [37]. Such solutions do not fit well with the size and purpose of the ALTER-EGO platform, where the introduction of heavy counterweights could bring about safety concerns.

Some consideration can also be given with regard to the design of the neck/head subsystem. The current solution does not ensure the following of the pilot's head trajectory perfectly (see the "Operating Modes" section). At the moment, however, this does not prevent the pilot from operating the robot in a satisfactory way. We believe that a more anthropomorphic design of the kinematic structure (i.e., at least 3 DoF configured as a spherical joint [15]) could enable a better performance in terms of both vision capabilities and user experience (by reducing the typical motion sickness that can occur after intense use of a VR system).

Conclusions

In this article, we presented ALTER-EGO, a dual-arm mobile platform developed using soft robotic technologies for the actuation and manipulation layers. Features resulting from this kind of technology, such as flexibility, adaptivity, and robustness, allow ALTER-EGO to interact with the environment and objects and provide improved safety when the robot is in proximity to humans. An overview of ALTER-EGO's mechatronic design, pilot interface, and core and high-level functions was presented. Most of the hardware and software technologies adopted, developed, and explicitly designed for ALTER-EGO are distributed under an open source framework and available on the NMMI website. The platform validation was performed both inside and outside the lab and involved several tasks. In particular, the house-simulation scenario demonstrated the potential of ALTER-EGO in a real-life situation. Future work will be devoted to investigating the role of haptic feedback interfaces as well as studying the platform's extensive use in different fields.

Acknowledgments

We thank Cristiano Petrocelli, Gaspare Santaera, Mattia Poggiani, Michele Maimeri, Manuel Barbarossa, Vinicio Tincani, and Ashwin Vasudevan for their work on the design and implementation of the ALTER-EGO robot. We also thank Grazia Zambella, Alessandro Palleschi, and Luca Bonamini for their help with the experimental activities.

References

[1] D. Gouaillier et al., "Mechatronic design of NAO humanoid," in *Proc. IEEE Int. Conf. Robotics and Automation (ICRA)*, 2010, pp. 3304–3309.

[2] E. Guizzo, "A robot in the family," *IEEE Spectr.*, vol. 52, no. 1, pp. 28–58, 2014. doi: 10.1109/MSPEC.2015.6995630.

[3] A. Parmiggiani et al., "The design and validation of the R1 personal humanoid," in *Proc. IEEE/RSJ Int. Conf. Intelligent Robots and Systems (IROS)*, 2017, pp. 674–680.

[4] F. Negrello et al., "Humanoids at work: The WALK-MAN robot in a postearthquake scenario," *IEEE Robot. Autom. Mag.*, vol. 25, no. 3, pp. 8–22, 2018.

[5] G. Nelson et al., "PETMAN: A humanoid robot for testing chemical protective clothing," *J. Robot. Soc. Jpn.*, vol. 30, no. 4, pp. 372–377, 2012.

[6] J. Englsberger et al., "Overview of the torque-controlled humanoid robot TORO," in *Proc. IEEE-RAS Int. Conf. Humanoid Robots*, 2014, pp. 916–923.

[7] C. Della Santina et al., "The quest for natural machine motion: An open platform to fast-prototyping articulated soft robots," *IEEE Robot. Autom. Mag.*, vol. 24, no. 1, pp. 48–56, 2017.

[8] M. Garabini, C. D. Santina, M. Bianchi, M. Catalano, G. Grioli, and A. Bicchi, "Soft robots that mimic the neuromusculoskeletal system," in *Converging Clinical and Engineering Research on Neurorehabilitation II*. J. Ibáñez, J. González-Vargas, J. Azorín, M. Akay, and J. Pons, Eds. New York: Springer-Verlag, 2017, pp. 259–263.
[9] A. Ajoudani, N. Tsagarakis, and A. Bicchi, "Tele-impedance: Teleoperation with impedance regulation using a body–machine interface," *Int. J. Robot. Res.*, vol. 31, no. 13, pp. 1642–1656, 2012.
[10] B. Siciliano, L. Sciavicco, L. Villani, and G. Oriolo, *Robotics: Modelling, Planning and Control*. London: Springer-Verlag, 2010.
[11] H. Culbertson, S. B. Schorr, and A. M. Okamura, "Haptics: The present and future of artificial touch sensation," *Annu. Rev. Control, Robot., Auton. Syst.*, vol. 1, no. 1, pp. 385–409, 2018.
[12] M. Stilman, J. Olson, and W. Gloss, "Golem Krang: Dynamically stable humanoid robot for mobile manipulation," in *Proc. IEEE Int. Conf. Robotics and Automation (ICRA)*, 2010, pp. 3304–3309.
[13] S. R. Kuindersma, E. Hannigan, D. Ruiken, and R. A. Grupen, "Dexterous mobility with the ubot-5 mobile manipulator," in *Proc. IEEE Int. Conf. Advanced Robotics*, 2009, pp. 1–7.
[14] G. Zambella et al., "Dynamic whole-body control of unstable wheeled humanoid robots," *IEEE Robot. Autom. Lett.*, vol. 4, no. 4, pp. 3489–3496, 2019.
[15] S. Mghames, M. G. Catalano, A. Bicchi, and G. Grioli, "A spherical active joint for humanoids and humans," *IEEE Robot. Autom. Lett.*, vol. 4, no. 2, pp. 838–845, 2019.
[16] W. An and Y. Li, "Simulation and control of a two-wheeled self-balancing robot," in *Proc. IEEE Int. Conf. Robotics and Biomimetics (ROBIO)*, 2013, pp. 456–461.
[17] C. Xu, M. Li, and F. Pan, "The system design and LQR control of a two-wheels self-balancing mobile robot," in *Proc. Int. Conf. Electrical and Control Engineering*, 2011, pp. 2786–2789.
[18] S. Fani, K. D. Blasio, M. Bianchi, M. G. Catalano, G. Grioli, and A. Bicchi, "Relaying the high frequency contents of tactile feedback to robotic prosthesis users: Design, filtering, implementation and validation," *IEEE Robot. Autom. Lett.*, vol. 4, no. 2, pp. 926–933, 2019.
[19] M. V. Damme et al., "Estimating robot end-effector force from noisy actuator torque measurements," in *Proc. IEEE Int. Conf. Robotics and Automation (ICRA)*, 2011, pp. 1108–1113.
[20] M. Labbe and F. Michaud, "Online global loop closure detection for large-scale multi-session graph-based SLAM," in *Proc. IEEE/RSJ Int. Conf. Intelligent Robots and Systems*, 2014, pp. 2661–2666.
[21] M. S. Arulampalam, S. Maskell, N. Gordon, and T. Clapp, "A tutorial on particle filters for online nonlinear/non-Gaussian Bayesian tracking," *IEEE Trans. Signal Process.*, vol. 50, no. 2, pp. 174–188, 2002.
[22] R. Coulter, "Implementation of the pure pursuit path tracking algorithm," Carnegie Mellon Univ., Pittsburgh, PA, Rep. CMU-RI-TR-92-01, 1992.
[23] S. O. Madgwick, A. J. Harrison, and R. Vaidyanathan. "Estimation of IMU and MARG orientation using a gradient descent algorithm," in *Proc. IEEE Int. Conf. Rehabilitation Robotics (ICORR)*, 2011, pp. 1–7.
[24] S. Fani et al., "Simplifying telerobotics: Wearability and teleimpedance improves human-robot interactions in teleoperation," *IEEE Robot. Autom. Mag.*, vol. 25, no. 1, pp. 77–88, 2018.
[25] N. Colella, M. Bianchi, G. Grioli, A. Bicchi, and M. G. Catalano, "A novel skin-stretch haptic device for intuitive control of robotic prostheses and avatars," *IEEE Robot. Autom. Lett.*, vol. 4, no. 2, 2019.
[26] iRobot, "If it is not iRobot, it is not a Roomba." Accessed on: Nov. 5, 2019. [Online]. Available: https://www.irobot.it/roomba
[27] Fernarbeiter. Accessed on: Nov. 5, 2019. [Online]. Available: http://www.fernarbeiter.de/en/
[28] DARPA, "Our research." Accessed on: Nov. 5, 2019. [Online]. Available: https://www.darpa.mil/program
[29] XPRIZE, "Anywhere is possible." Accessed on: Nov. 5, 2019. [Online]. Available: https://avatar.xprize.org/prizes/avatar
[30] XPRIZE, "Guidelines." Accessed on: Nov. 5, 2019. [Online]. Available: https://avatar.xprize.org/prizes/avatar/guidelines
[31] NMMI. Accessed on: Nov. 5, 2019. [Online]. Available: www.naturalmachinemotioninitiative.com
[32] GitHub, "NMMI/EGO." Accessed on: Nov. 5, 2019. [Online]. Available: https://github.com/NMMI/EGO
[33] Stereo Labs. Accessed on: Nov. 5, 2019. [Online]. Available: https://www.stereolabs.com/
[34] GitHub, "Facebook research/detectron." Accessed on: Nov. 5, 2019. [Online]. Available: https://github.com/facebookresearch/detectron
[35] ROS.org, "Aruco." Accessed on: Nov. 5, 2019. [Online]. Available: http://wiki.ros.org/aruco
[36] Nintendo, "Wii." Accessed on: Nov. 5, 2019. [Online]. Available: https://www.nintendo.it/Wii/Wii-94559.html
[37] Boston Dynamics, "Handle." Accessed on: Nov. 5, 2019. [Online]. Available: www.bostondynamics.com/handle

Gianluca Lentini, Istituto Italiano di Tecnologia, Genoa, Italy, and Department of Information Engineering, Research Center Enrico Piaggio, University of Pisa, Italy. Email: gianluca.lentini@iit.it.

Alessandro Settimi, Department of Information Engineering, Research Center Enrico Piaggio, University of Pisa, Italy. Email: alessandro.settimi@for.unipi.it.

Danilo Caporale, Department of Information Engineering, Research Center Enrico Piaggio, University of Pisa, Italy. Email: d.caporale@centropiaggio.unipi.it.

Manolo Garabini, Department of Information Engineering, Research Center Enrico Piaggio, University of Pisa, Italy. Email: manolo.garabini@gmail.com.

Giorgio Grioli, Istituto Italiano di Tecnologia, Genoa, Italy. Email: giorgio.grioli@iit.it.

Lucia Pallottino, Department of Information Engineering, Research Center Enrico Piaggio, University of Pisa, Italy. Email: lucia.pallottino@unipi.it.

Manuel G. Catalano, Istituto Italiano di Tecnologia, Genoa, Italy. Email: manuel.catalano@iit.it.

Antonio Bicchi, Istituto Italiano di Tecnologia, Genoa, Italy, and Department of Information Engineering, Research Center Enrico Piaggio, University of Pisa, Italy. Email: antonio.bicchi@iit.it.